Probing the relationship between the scales of space and time in an entangled polymer network with an oscillating nanotip

2003 J. Phys.: Condens. Matter 15 6167

(http://iopscience.iop.org/0953-8984/15/36/307)

INSTITUTE OF PHYSICS PUBLISHING JOURNAL OF PHYSICS: CONDENSED MATTER

J. Phys.: Condens. Matter **15** (2003) 6167–6177 PII: S0953-8984(03)59652-7

Probing the relationship between the scales of space and time in an entangled polymer network with an oscillating nanotip

F Dubourg, J P Aimé[1], S Marsaudon, G Couturier and R Boisgard

CPMOH University Bordeaux I, 351 Cours de la Libération F-33405, Talence, France

E-mail: jpaime@cpmoh.u-bordeaux1.fr

Received 12 February 2003, in final form 15 July 2003
Published 29 August 2003
Online at stacks.iop.org/JPhysCM/15/6167

Abstract

The dynamical behaviour of an entangled network, a melt made of long polymer chains, with an oscillating nanotip, is investigated to provide evidence for a close relationship between the spatial scale and dynamics of the network, from the molecular to the mesoscopic scale. The experimental results show how a dynamic force microscope is able to discriminate between slow and fast relaxation processes related to molecular motion at different scales. In particular, it is shown that within a very small variation of the tip indentation depth, a few ångströms, the relaxation times involved in the process of dissipation vary by more than three orders of magnitude.

(Some figures in this article are in colour only in the electronic version)

1. Introduction

The dynamics of flexible polymer chains in a melt provides a unique combination of viscous and elastic behaviour, in particular when the chains are long enough to build an entangled network [1]. Viscous properties are dependent on the timescale and spatial scale of observation. There is a close relationship between the spatial scale and the dynamics of the flexible long chains. In general, the fast dynamics corresponds to motion on a small scale, while the slow dynamics reflects the motion over a larger spatial scale. These features, influenced by the chain connectivity, are very similar for polymer chains of various chemical structures. This universality leads to dynamic scaling laws for a polymer melt that may also be useful for understanding the viscoelastic behaviour at the nanometre scale.

A polymer melt is a network made of physical entanglements with an average distance ξ between entanglements. When spheres of diameter $\phi < \xi$ move in the network, only a few monomer units are involved in the motion and the mobility is high. For $\phi > \xi$, the sphere

[1] Author to whom any correspondence should be addressed.

0953-8984/03/366167+11$30.00

motion involves the chain connectivity, and the mobility is expected to decrease drastically [2]. Therefore even for a sphere diameter of a few nanometres, the viscosity must rise to reach a value close to the macroscopic value. Similarly, the viscoelastic response should exhibit a sharp dependence as a function of the spatial scale.

The present work is based on the idea of immersing small oscillating particles of different sizes, then relating changes of the oscillation behaviour of the particles to the viscoelastic properties of the medium. To do this, a dynamic force microscope is used, adopting the conceptually simple idea that the variation of the contact area between the tip and the sample as a function of the tip indentation depth is similar to the variation of the radius of a sphere.

2. Material and method

The experiments were performed with an atomic force microscope in the dynamic mode using the frequency modulation technique (FM-AFM) [3–6]. With a FM-AFM, the oscillation amplitude of the cantilever is kept constant and the driving force needed to keep this oscillation amplitude constant provides a direct measurement of the damping coefficient. Technically, the additional force that preserves a stationary state of the nanotip oscillation is given by the error signal, or damping signal, of the automatic gain control (AGC) [6]. The damping signal gives the amount of additional energy dissipated in the medium as a function of the indentation depth and in turn provides information on its viscoelastic properties.

The tip–surface interaction governs the oscillation behaviour of the AFM; thus it is a function of the size and shape of the tip. Therefore, when one wants to perform comparative studies, it is necessary to keep the tip size constant throughout the experiment. In the present study, because at long timescales a polymer melt behaves as a liquid, we need to avoid any wetting of the tip with the polymer chains. The long time behaviour of an entangled network is determined by the reptation time of the chain inside the network. The reptation time scales like $\tau_{rep} \approx M_w^{3.6}$ [1], where M_w is the molecular weight of the chain, so τ_{rep} is often larger than a millisecond [1]. Therefore, when the AFM tip oscillates at a frequency of a hundred kilohertz, the time during which the tip remains in the network is no greater than a microsecond and the polymer never has time to cover the tip as happens with the AFM static mode [7].

As shown in preceding papers [8, 9], with the constant frequency mode (also called the tapping mode), the quality factor is a key parameter. In particular, the effective surface local stiffness is proportional to the product of the quality factor and the local stiffness. Therefore, with a high quality factor, even a soft sample may appear as a hard one and the tapping mode becomes inappropriate for investigating a wide range of tip indentation depths. In contrast, the FM-AFM keeps the oscillation amplitude constant at any indentation depth as long as the AGC electronic loop is able to provide the additional energy [6]. When this condition is fulfilled, the conservative forces, through the resonance frequency shift, and the dissipating forces, through the change of the damping signal [4–6], are separately and simultaneously recorded. The machine is a hybrid one, with which either the FM-AFM or the tapping mode can be used [6]. The cantilever has a resonance frequency of 175 kHz and a supersharp tip, SSS-NCL. A supersharp tip is identified by having an apex radius of about 3–5 nm [10]. In the present work, the size of the tip is evaluated *in situ* by recording an approach curve, in the tapping mode, in air on a silica surface heated to 400 °C to eliminate the water layer [11]. From the approach curves it is deduced that the SSS-NCL tips were always smaller than the usual ones, referred to as NCL, used for tapping or non-contact AFM. A good NCL tip, i.e. one with a small radius at the apex, shows a transition from a dominant repulsive regime to an attractive one with a oscillation amplitude ranging between 5 and 10 nm (see [8] for more detailed information). When the dominant attractive regime occurs with an oscillation

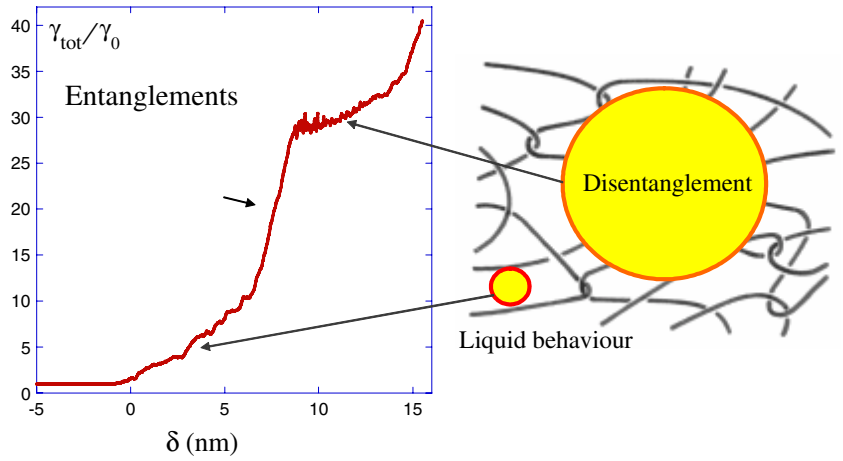

Figure 1. A typical normalized damping curve recorded when the tip was dipped into the polyisoprene. The x axis gives the indentation depth δ; γ_0 is the damping coefficient of the AFM oscillator when the tip is far from the surface. The measured damping coefficient γ_{tot} follows the linear relationship $\gamma_{tot} = \gamma_0 + \gamma_{int}$. The oscillation amplitude is $A = 50$ nm. Three regimes are identified as shown with the scheme of an entangled polymer network.

amplitude larger than 10 nm, since the effective time during which the tip interacts with the surface scales as $\sqrt{1/A}$ (see below), this result means that the size of the tip is large enough to make the attractive regime dominant even at a rather large amplitude. In that case the cantilever is removed. With an SSS-NCL, the transition between the two regimes often occurs with oscillation amplitudes smaller than 5 nm. Note that this method is helpful for verifying that the size of the tip does not vary over the whole experiment.

Experiments are performed in a secondary vacuum (2×10^{-7} Torr) providing a high quality factor, $Q = 23\,000$, when the tip does not interact with a surface. So high a quality factor gives a sensitivity on the damping curve of about $k_B T$ with $T = 300$ K and k_B the Boltzmann constant.

The polymer network used was a polyisoprene of molecular weight $M_w = 205$ kDa with a polydispersity $M_w/M_n = 1.05$. The glass transition temperature is 200 K, the melting temperature 308 K [12]—close to that of the present experiment: 303 K. Since the sample behaves as a liquid, a small basin was used to avoid a flow of the polymer during the experiment.

The experiments were as follows. For a given oscillation amplitude we recorded an approach curve at a fixed X, Y location on the surface. The approach curve was obtained by moving the sample along the vertical axis Z. For each curve, the duration was 10 s with a total vertical displacement varying between 20 and 40 nm. Typical variations of the normalized damping signal versus the tip indentation are shown in figure 1. We only know the vertical displacement of the surface; thus the absolute value of the distance between the tip and the sample can only be evaluated with a model. The absolute value is deduced from a fit of the resonance frequency shift curve in the attractive regime with an analytical expression taking into account the van der Waals interaction [13] (figure 2). The uncertainty, estimated as a few ångströms, is negligible compared to values of the indentation depths.

3. Experimental results and analysis

When the tip dips into the melt, the damping coefficient γ_{tot} becomes the sum of the intrinsic damping coefficient γ_0 and the damping coefficient γ_{int} related to the additional dissipation [14–16]. The damping coefficient γ_{int} is an explicit function of the indentation

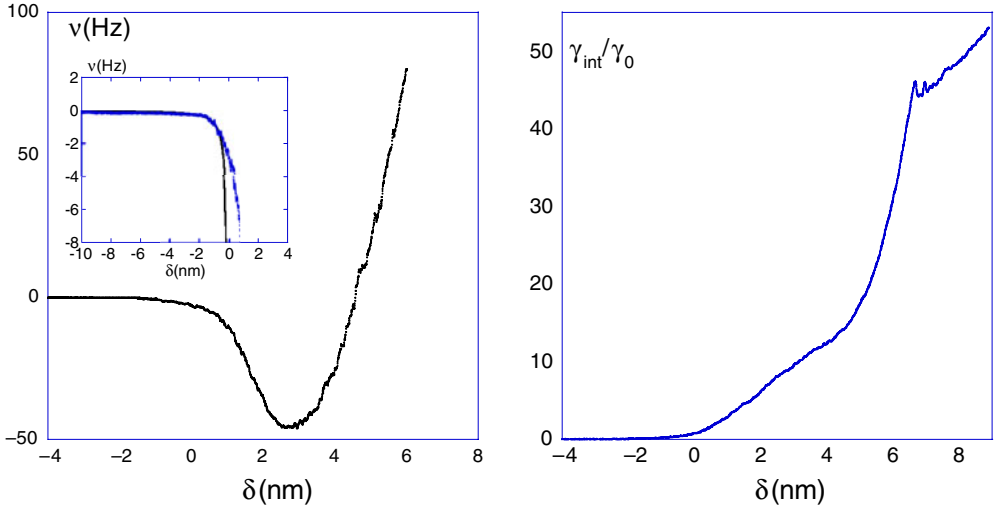

Figure 2. Variation of the resonance frequency shift (left) and of the damping signal (right) as a function of the tip–surface distance. The resonance frequency ν_0 is subtracted; the oscillation amplitude is $A = 25$ nm. The location of the surface, corresponding to a null indentation, is determined with a fit of the resonance frequency shift curve (inset). The continuous curve is a theoretical curve in which only the attractive interaction is considered [13].

depth δ: $\gamma_{\rm int} = \gamma_{\rm int}(\delta)$. The damping curves show three domains (figures 1 and 3). At small indentation, the dissipation is rather low and increases smoothly, then follows an abrupt increase within a few ångströms' variation. At larger indentations, the last part of the curves again increases smoothly or exhibits a plateau-like behaviour. A qualitative explanation of this non-regular behaviour can be readily given as follows: the low part of the curve corresponds to dissipation processes that only involve motion of segment chains with lengths smaller than the entanglement length. Then, the abrupt increase corresponds to indentation that involves entanglements, and the last part includes contributions due to significant disentanglements of the network. Since at large indentation depths disentanglements of the network occur, one needs to wait 5–10 min to recover a similar curve at the same X, Y location. Consequently, to avoid measurements in a strongly modified network structure, after each curve had been taken the surface was laterally displaced along either the X or Y axis; then a new damping curve was recorded with another oscillation amplitude. Damping curves recorded at four oscillation amplitudes are displayed in figure 4.

In this paper, we focus the analysis on the transition between the low part of the curve and the sharp increase. Starting from these experimental results, it is worth discussing first some technical aspects related to a nanorheological experiment performed with an AFM. In general, when one wants to investigate the viscoelastic properties of a material, it is very common to vary the excitation frequency or the shear rate. When an AFM cantilever is used, the available frequency range is limited and centred at the mechanical resonance frequency of the cantilever; nevertheless it remains possible to vary the shear rate through change of the oscillation amplitude. Typically, the time during which the tip dips into the network, hereafter called the residence time $\tau_{\rm res}$, to first order expansion scales as $\tau_{\rm res} \sim T\sqrt{\delta/A}$ where T is the oscillation period and A the oscillation amplitude. Consequently, for the same value of the indentation depth, the use of different oscillation amplitudes gives different residence times of the tip in the melt; in turn, this provides a way to discriminate between fast and slow relaxation processes.

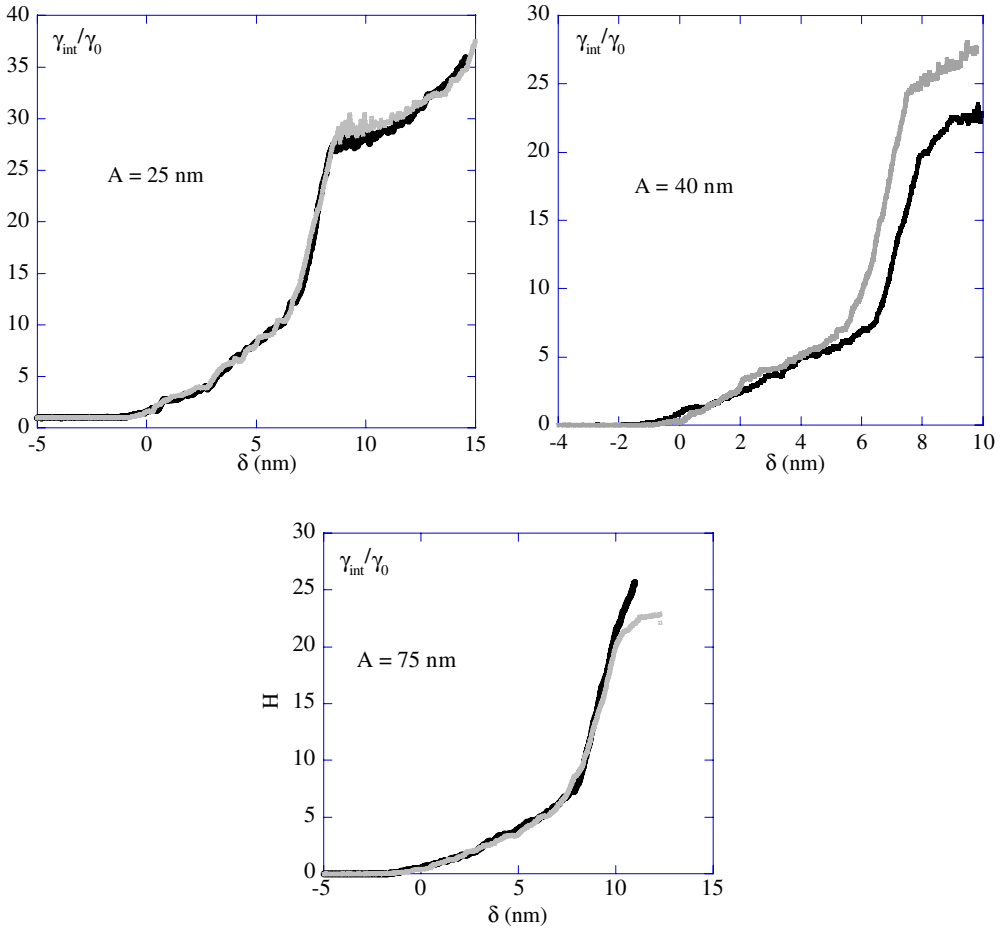

Figure 3. Several damping curves recorded at two different locations in the (X, Y) plane for different oscillation amplitudes. In a few cases the curves show a dispersed behaviour at the values of the indentation depth where the transition between the different regimes occurs. Whatever the location, the general features remain the same in agreement with the tapping images recorded in air showing an homogeneous mechanical behaviour [9].

We face a few difficulties in attempting to accurately describe the dipping process of an oscillating nanotip in a viscoelastic material. First, the sample excitation is made up of pulses of width $\tau_{\rm res}$ and the indentation depth temporal function is $\delta(t) = A\cos(\omega t) - D$ for $t \in [-\tau_{\rm res}/2, \tau_{\rm res}/2]$ and $\delta(t) = 0$ elsewhere, where D is the distance between the surface and the tip at rest and with the condition $A > D$. Therefore a Fourier series is required to describe the shear rate induced by the oscillating tip. Second, because a quantitative analysis of the additional dissipation due to a viscoelastic medium or a viscous fluid requires an accurate knowledge of the tip shape and size at the nanometre scale [15], an accurate description of the deformation gradient induced by the tip motion is far from being obvious. To avoid this latter complication, a phenomenological approach is chosen, in which the tip motion induces a simple shear deformation.

Similarly to what was done for the calculation of the dissipation induced by the growth of a nanoprotuberance [16], we use an elementary Maxwell model to predict the general

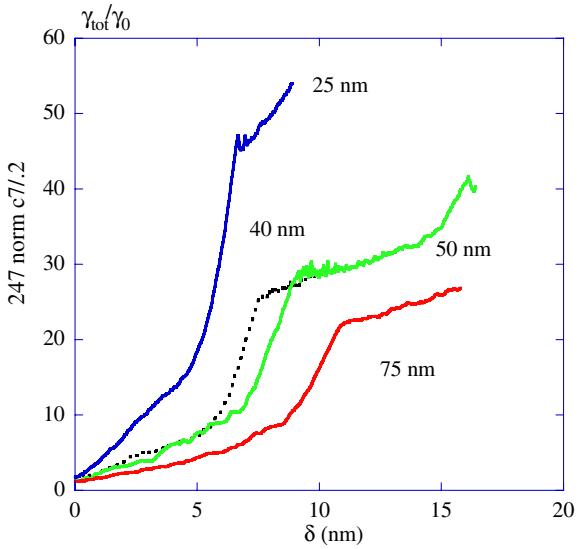

Figure 4. The damping curves are recorded at different X, Y locations in the sample for four oscillation amplitudes $A = 25$, 40, 50 and 75 nm. At a given indentation depth, the variation of the oscillation amplitude induces change of the residence time in the polymer. A consequence is that the transition between the two regimes occurs at different indentation depths.

trends [17]. The Maxwell unit is built with a dashpot and a spring in series. When an oscillating shear is applied, the constraint σ required to maintain a stationary oscillation is $\sigma(t) = -\int_{-\infty}^{t} G(t-t')\dot{\gamma}(t')\,\mathrm{d}t'$ with $G(t) = \eta/\tau_s \exp(-t/\tau_s)$ the material relaxation modulus, τ_s the sample relaxation time, $\dot{\gamma}$ the shear rate and η the zero frequency viscosity.

A first step is the evaluation of the deformation gradient γ and the associated shear rate $\dot{\gamma}$ generated by the tip motion. Here we set $\gamma \sim \delta/\phi$ and $\dot{\gamma} \sim \dot{\delta}/\phi$, where ϕ is the diameter of the area of the contact between the tip and the polymer. Such an approximation means that the induced deformation vanishes over the length ϕ. Thus a nanorheological experiment gives a large deformation gradient of about the unity and, since the residence time is around the microsecond, the shear rate is also large with $\dot{\gamma} \sim 10^6\ \mathrm{s}^{-1}$. While this value is rather large when it is compared to what can be done with rheological experiments performed at a macroscopic scale, it remains a small value for usual timescales in the nanometre domain [16, 18]. For example, in [15] it was demonstrated that for a complex fluid, because of the nanometre scale size, the fact that the tip vibrates at 200 kHz does not matter and the Stokes equation applies. Similarly, for a viscoelastic medium one can demonstrate that the contributions of acoustic waves and phonons are negligible [16, 18]. The main physical reason is that the volume of material investigated is too small and the oscillation frequency is too low. For example, even with a very large tip of micrometre size, one needs an oscillator vibrating at the gigahertz level to obtain a detectable amount of damping signal related to acoustic waves. Therefore, only viscous processes such as those investigated in the present work are able to contribute to the damping signal, provided that their timescales are within the range of the characteristic times of the AFM oscillator as discussed below.

The next step is to calculate the additional energy loss per period:

$$E_T^{\mathrm{diss}} = S\int_0^T \sigma(t)\dot{\delta}\,\mathrm{d}t \tag{1}$$

where S is the contact surface scaling like the product $\phi\delta$. Note that the choice of the shape of the tip, spherical or conical, and the choice of the expression for the deformation gradient γ have an influence on the δ power law of the additional energy loss but not on the A power law. Since, in this work, we are mostly concerned with the A power law dependence, the assumptions given above are not of primary importance. Applying the Fourier transform and after some calculations using the relation $\eta'(\omega) = G''(\omega)/\omega$ with G'' the loss modulus [17] and the expression for the total energy dissipated per period $E_T^{\text{diss}} = \pi\omega(\gamma_0 + \gamma_{\text{int}})A^2$ one gets the general result, omitting numerical factors:

$$\gamma_{\text{int}} \propto \frac{\delta}{(\omega A)^2} \sum_{n=1}^{\infty} \eta'(n\omega)\dot{\delta}_n^2 \tag{2}$$

where $\eta'(n\omega) = \eta/(1 + (\tau_s n\omega)^2)$ is the real part of the complex viscosity at the frequency $n\omega$ and $\dot{\delta}_n = \delta_n n\omega$ are the Fourier components of $\dot{\delta}(t)$; $\omega = 2\pi/T$ is the frequency cycle of the AFM oscillator of oscillation period T. Note that $\eta'\delta$ scales as the friction coefficient γ at the indentation depth δ.

One has to calculate the Fourier components $\dot{\delta}_n$, then evaluate the sum in equation (2). An exact calculation can only be performed numerically (see below). However, useful analytical expressions are obtained by making assumptions similar to those given in [16]. A first one consists in replacing the Fourier components δ_n by the product $\delta\tau_{\text{res}}/T$ for $n \leqslant n_0 = \sqrt{A/\delta} \sim (\tau_{\text{res}}/T)^{-1}$ and $\delta_n = 0$ for $n > n_0$, with n_0 an integer number corresponding to the highest harmonic involved in the interaction. Thus, $\dot{\delta}_n \sim n\omega\delta\tau_{\text{res}}/T$ up to $n = n_0$ and the sum in equation (2) is truncated at the n_0 value; we get

$$\gamma_{\text{int}} \propto \frac{1}{(\omega A)^2}\frac{\delta^4}{A}\sum_{n=1}^{n_0}(n\omega)^2\eta'(n\omega). \tag{3}$$

A second approximation is based on examining the two asymptotic behaviours, fast and slow relaxation processes, from which power law predictions are readily obtained:

(i) Fast relaxation processes, $\tau_s n_0\omega \ll 1$ or $\tau_s \ll \tau_{\text{res}}$: from equation (3) and the expression for $\eta'(n\omega)$ one gets

$$\gamma_{\text{int}} \propto \eta\frac{\delta^{5/2}}{A^{3/2}}. \tag{4}$$

The prediction corresponding to fast relaxation processes must recover some of the results obtained when the medium behaves as a liquid. Equation (4) gives the same power laws as the one derived with the Stokes law for a simple liquid [15]. When the Rouse modes are included, the indentation depth dependence is more pronounced leading to the power law $\delta^{7/2}$ [15].

(ii) Slow relaxation processes, $\tau_s\omega \gg 1$:

$$\gamma_{\text{int}} \propto \frac{\eta}{\tau_s^2\omega^2}\frac{\delta^{7/2}}{A^{5/2}}. \tag{5}$$

Equations (4) and (5) predict that the power law dependence on the oscillation amplitude depends on the timescale of the sample characteristic relaxation time. As a result, a simple algebraic transformation is sufficient to discriminate between the two regimes: fast and slow relaxation processes. The characteristic times of the relaxation processes involved in the additional dissipation will be readily identified by multiplying the experimental data by the power law dependences $A^{3/2}$ and $A^{5/2}$. The results are shown in the figures 5 and 6. When the experimental data are multiplied by $A^{3/2}$, the low parts of the curves, corresponding to the small indentations, gather together, showing that the relaxation times of the processes

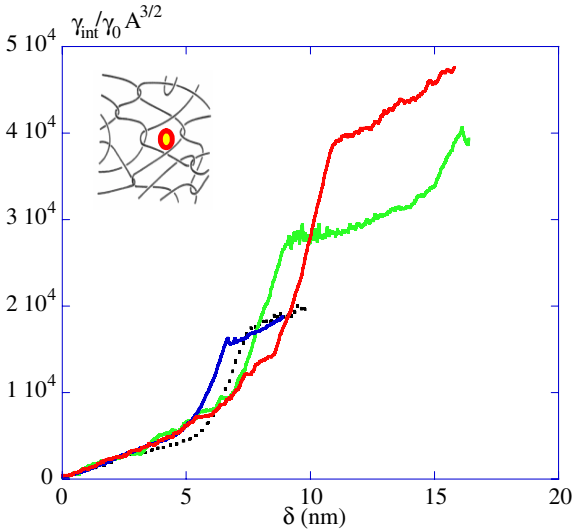

Figure 5. The same data as shown in figure 3 with the y axis multiplied by the power law $A^{3/2}$.

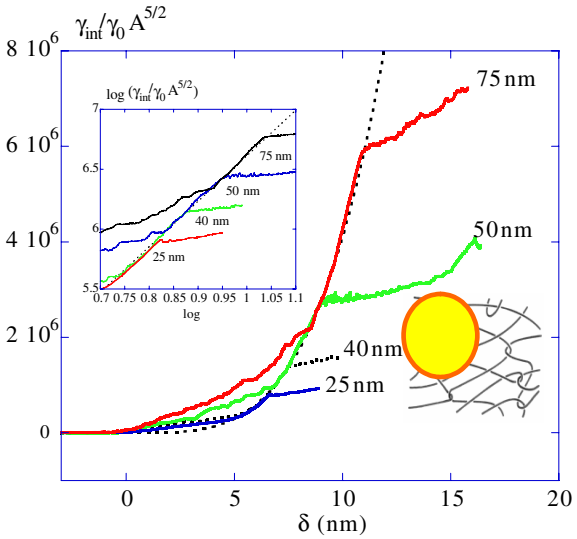

Figure 6. The same data as shown in figure 3 with the y axis multiplied by the power law $A^{5/2}$. The inset shows a log–log plot of the part of the curves corresponding to the slow relaxation regime. The slope found is 3.8, in good agreement with the prediction (equation (5)).

induced in the network are much smaller than the residence times. When the experimental data are multiplied by $A^{5/2}$, all the abrupt increases of the dissipation align. On increasing the indentation depth by a fraction of nanometre, the relaxation processes switch from fast to slow relaxation times. The log–log plot shown in the inset of figure 6 gives a slope of 3.8 in good agreement with the prediction (equation (5)).

At large indentation depths, the slow relaxation processes prevail. The abrupt variation, from relaxation processes faster than the microsecond to relaxation processes governed by

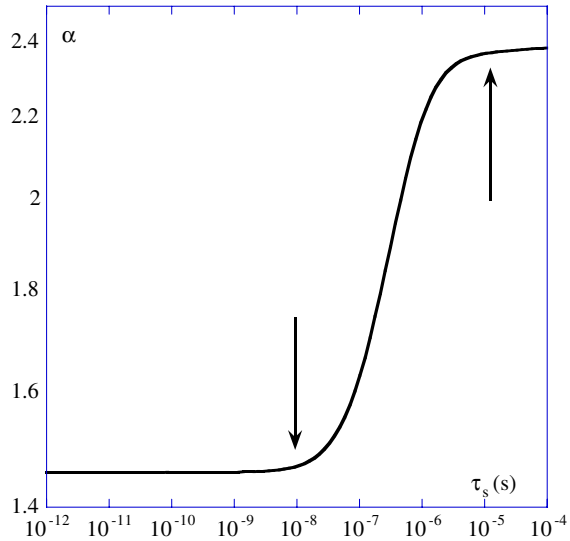

Figure 7. Exact computation of the exponent α of the amplitude power law dependence $A^{-\alpha}$ of $\gamma_{\rm int}$ as a function of the value of the sample relaxation times $\tau_{\rm s}$ (seconds). The numerical calculation is based on equation (2) with the Fourier coefficients δ_n given by equation (6). The parameters are: $\nu_0 = 180$ kHz, $\delta = 20$ nm, $\eta = 10$ Pa s. To calculate the power law, the amplitudes are varied from $A = 20$ to 230 nm. For fast relaxation times, $\tau_{\rm s} < 10^{-8}$ s, $\alpha = 1.46$; for slow relaxation times, $\tau_{\rm s} > 10^{-5}$ s, $\alpha = 2.37$. The numerical values are close to the ones calculated with the simplified assumptions (equations (4) and (5)): 3/2 and 5/2 respectively.

relaxation times involving the network, occurs within an increase of the indentation depth of only a few ångströms.

Due to the assumptions employed to verify the amplitude power law dependences on the asymptotic behaviours, it is worth performing an exact computation. The numerical calculation is based on equation (2) with the exact Fourier coefficients δ_n given by

$$\delta_n = \frac{A}{\pi}\left\{\frac{\sin[(n-1)\omega\tau_{\rm res}/2]}{n-1} + \frac{\sin[(n+1)\omega\tau_{\rm res}/2]}{n+1}\right\} - \frac{2D}{\pi}\frac{\sin(n\omega\tau_{\rm res}/2)}{n}. \tag{6}$$

The numerical calculation is performed up to $n = 300$. In figure 7 we show the variation of the exponent of the amplitude power law as a function of the sample relaxation time at a fixed indentation depth. The numerical results show that relaxation processes lead to a power law $A^{-1.46}$ when the relaxation times are of the order of or faster than 10 ns, while relaxation processes give a power law $A^{-2.37}$ when the relaxation times are greater than 10^{-5} ns. Consequently, the experimental results indicate that within a very tiny variation of the indentation depth (a few ångströms) the relaxation times involved in the dissipation processes vary by, at least, three orders of magnitude. This abrupt change confirms that the network contribution prevails in the transition zone.

4. Discussion

For fast relaxation times, i.e. ones for which the network contribution is negligible, the Rouse model [1] gives an evaluation of the relaxation time of a chain portion with an end to end distance of 3 nm, just below the mesh size of the network. For the polyisoprene, with a monomeric friction coefficient of 10^{-11} N m^{-1} s [17], one gets $\tau_{3\ {\rm nm}} = 5 \times 10^{-8}$ s in agreement with the

present experimental results. Faster relaxation modes also contribute to dissipation processes; for example, including the Rouse modes leads to a double sum in equation (3). When the longest relaxation time is about 10^{-8} s, the dissipation curve computed numerically with the double sum and the one calculated with equation (4) give the same evolution. The main difference concerns numerical factors. In other words a more refined analysis helps one to obtain more quantitative information, still keeping in mind that the tip shape also matters.

For slower relaxation processes, the contribution of the network connectivity is more difficult to evaluate because almost nothing is known regarding the dynamical behaviour on physical entanglement. The reptation time of a polyisoprene chain of molecular weight 205 kDa is deduced from the know value at $M_w = 357$ kDa, $\tau_{rep} = 1$ s [19]. Using the scaling law $\tau_{rep} \approx M_w^{3.6}$, the reptation time is $\tau_{rep}(M_w = 205\ \text{kDa}) \approx 0.14$ s. The shortest network relaxation time can be evaluated with a phenomenological mode analysis [20]: $\tau_{net} = \tau_{rep}/1.5^N$, where the maximum value N corresponds to the higher mode of the physical entanglement and is taken to be $N = 13$. Using $N = 13$, one gets $\tau_{net} = 5 \times 10^{-4}$ s, at least an order of magnitude greater than the value needed to observe the $A^{-5/2}$ power law. In the present state of our experimental results one cannot say whether or not faster relaxation times are involved in the network. Our data analysis shows that relaxation times of only a few 10 μs can also produce the power law $A^{-5/2}$.

The present results indicate that, even at a high excitation frequency and at the molecular scale, viscoelastic properties can be qualitatively understood with the help of dynamic scaling laws that discriminate between molecular motion and the influence of the network connectivity. A more quantitative analysis of the scaling laws would investigate the influence of the mesh size. This could be done through studies of the effect of the disentanglement (increase of the mesh size) and the ageing effect (re-formation of the network). Such experiments are currently under way. The present work shows the ability of an AFM oscillator to discriminate between the dynamics of a complex system at different scales, in particular when a network structure induces a long range hydrodynamic interaction.

References

[1] Doi M and Edwards S F 1986 *The Theory of Polymer Dynamics* (Oxford: Oxford Science Publications)
de Gennes P G 1991 *Scaling Concept in Polymer Physics* 4th edn (Ithaca, NY: Cornell University Press)
[2] Brochard Wyart F and de Gennes P G 2000 *Eur. Phys. J.* E **1** 93
[3] Albrecht T R, Grütter P, Horne D and Rugar D 1991 *J. Appl. Phys.* **69** 668
[4] Lantz M A *et al* 2000 *Phys. Rev. Lett.* **84** 2642
Loppacher Ch *et al* 2000 *Phys. Rev.* B **62** 16944
[5] Gauthier M and Tsukada M 1999 *Phys. Rev.* B **60** 11716
Dürig U 2000 *New J. Phys.* **2** 5.1
Couturier G *et al* 2001 *Eur. Phys. J.* B **15** 141
[6] Couturier G *et al* 2001 *J. Phys. D: Appl. Phys.* **34** 1266
[7] Frétigny C and Basire C 1997 *J. Appl. Phys.* **82** 43
[8] Nony L, Boisgard R and Aimé J P 1999 *J. Chem. Phys.* **111** 1615
[9] Dubourg F, Aimé J P, Couturier G and Salardenne J 2003 *Eur. Phys. Lett.* **62** 671
[10] www.nanoandmore.fr and private communication
[11] Nony L, Cohen-Bouhacina T and Aimé J P 2001 *Surf. Sci.* **499** 152
Bouhacina T, Desbat B and Aimé J P 2000 *Tribol. Lett.* **9** 111
[12] Dalai E N, Taylor K D and Philips P J 1983 *Polymer* **24** 1623 (Polymer Standards Service, Postfach 3368, D-55023 Mainz)
[13] Aimé J P, Boisgard R, Nony L and Couturier G 1999 *Phys. Rev. Lett.* **82** 3388
[14] Cleveland J, Anczycowski B, Schmid A and Elings V 1998 *Appl. Phys. Lett.* **72** 2613
[15] Dubourg F, Aimé J P, Marsaudon S, Boisgard R and Leclère P 2001 *Eur. Phys. J.* E **6** 49
[16] Boisgard R, Aimé J P and Couturier G 2002 *Surf. Sci.* **511** 171

[17] Ferry J 1980 *Viscoelastic Properties of Polymer* vol 3 (New York: Wiley)
Bird R B, Armstrong R C and Hassag O 1987 *Fluid Mechanics* vol 1 (New York: Wiley)
[18] Dürig U 1999 *Surf. Interface Anal.* **27** 467
[19] Bero C A and Roland C M 1996 *Macromolecules* **29** 1562
[20] Inoue T, Yen Y and Osaki K 2002 *Macromolecules* **35** 1770